Finite Element Analysis of Rectangular RC Beams Strengthened with FRP Laminates under Pure Torsion

Muhanad M. Majed[1], Mohammadreza Tavakkolizadeh*[2], Abbas A. Allawi[3]

1- Graduate Student, Department of Civil Engineering, Ferdowsi University of Mashhad, Iran.
E-mail: al-deraan9526411020@mail.um.ac.ir

2- Assistant Professor, Department of Civil Engineering, Ferdowsi University of Mashhad, Iran.
E-mail: drt@um.ac.ir

3- Professor, Department of Civil Engineering, University of Baghdad, Iraq.
E-mail: a.allawi@uobaghdad.edu.iq

Corresponding author: Mohammadreza Tavakkolizadeh, Department of Civil Engineering, Ferdowsi University of Mashhad, Iran.
E-mail: drt@um.ac.ir
Tel: +98 513 8806021

Finite Element Analysis of Rectangular RC Beams Strengthened with FRP Laminates under Pure Torsion

Abstract: Composite materials have attracted wide attention in structural engineering research as they present exceptional advantages when used to strengthen structural members. In this study, the behavior of rectangular reinforced concrete (RC) strengthened with fiber reinforced polymer (FRP) laminates under pure torsion was analyzed by ABAQUS Software program. The experimental data was obtained from existing literature on the subject. The contribution of FRP, as an external bonded reinforcement, to torsional response is studied in various practical strengthening configurations and the efficiency of each configuration was illustrated. The paper presents the method and requirements of material parameters identification for a concrete damage plasticity constitutive model. Good agreement in terms of torque–twist behaviors of concrete beams reinforced with FRP laminates before and after cracking was found. Steel and FRP reinforcement responses as well as crack patterns were achieved. The unique failure modes of all the specimens were modeled correctly as well. A parametric study was carried out after model validation by varying the number of FRP plies, concrete compressive strength, and FRP strip orientations. The results showed that the torsional capacity of strengthened RC beams improves by increasing the number of FRP plies and concrete compressive strength as expected. The parametric study showed no significant change in the torsional capacity of RC beams when it was strengthened with a 45-degree or with a 90-degree FRP laminate.

Keywords: Rectangular beam, Reinforced concrete, Torsion, FRP, Strengthening, Finite Element, Failure.

1. INTRODUCTION

Reinforced concrete (RC) members in a structure may be subjected to loads with magnitudes greater than those considered as design loads. Axial forces, shear forces, bending moments, torsional moments, or a combination of these effects are considered in the design of a safe structural member. In most design situations, bending moments and shear forces exert the primary effects, whereas the torsional moment is considered to have a secondary impact. Occasionally, torsional moments can exerts a primary effect in situations such as spandrel or curved beams.[1] Torsional strengthening of RC beams has been performed by several techniques such as steel plate jacketing, increasing cross-sections, and adding extra steel bars in the past.

Fiber reinforced polymer (FRP)s have been commonly used in other engineering fields such as automotive and aerospace industries. Exceptional mechanical and physical characteristics of FRP laminates make them attractive in structural engineering rehabilitation applications, especially for repair and strengthening of RC and masonry structures. The advantages of FRPs, such as their relatively high strength to weight ratio, high resistance in corrosive regions, and their easy-to-apply characteristic, have caused an interest in extending the application of this material for strengthening purposes.

Flexural strengthening of RC members with externally bonded FRP laminates has been addressed by several researchers in the past three decades.[2-6] A number of investigations have been conducted on the shear strengthening of RC beams as well.[7-12] Moreover, several investigations have been performed on axial load,[13-16] while the study of torsional strengthening of structural elements using FRPs has not received much attention.

Ghobarah et al.[1] examined RC beams with a rectangular cross-section strengthened with glass and carbon FRPs to improve torsional capacity. In that study, different strengthening schemes were evaluated and a simple design method was presented. Panchacharam and Belarbi[17] studied the influence of fiber

orientation, continuous full wrapping versus strips, three versus four sides strengthened longitudinally and complete wrap versus U-wrap. They suggested design equations for both cracking and ultimate torsional moments, which seemed to predict the experimental results very accurately. Salom et al.[18] tested six RC spandrel beams and the variables considered in that study included fiber orientation, composite laminates and the effect of anchoring system. The study proved that FRP laminates could increase the torsional capacity of concrete beams by over 70%. Hii and Al-Mahaidi[19] examined six RC beams and found that carbon fiber reinforced polymer (CFRP) increases both cracking and ultimate strength by 40% and 78% for box and solid sections, respectively. After testing beams that are strengthened with a CFRP laminates, Souza et al.[20] stated that structure reliability declined when torsion moment rose.

Very few researchers have focused on the numerical study of the behaviors of RC members under torsion. Majeed et al.[21] studied experimental and numerical works in an investigation for torsional strengthening of multicell box section RC girders with externally bonded CFRP strips. A numerical work was also carried out using nonlinear finite elements (FE) by using the DIANA software program, and good agreements in terms of torque–twist behavior, stress developed in steel and CFRP reinforcement, and cracking patterns were observed. The failure modes of all the samples were modeled correctly as well. A new method by using finite element analysis for demonstrating CFRP anchors was established by Sakin and Anil[22] in which it is concluded that there is a good agreement between experimental and modeled data.

Alabdulhady and Sneed[23] conducted a review on torsional strengthening of RC beams with externally bonded composites, wrapping methods, failure modes, and anchorage systems, and the accuracy of the existing numerical and analytical models was compared. Several FE software programs such as ABAQUS, DIANA, ANSYS, and LS-DYNA were used for numerical evaluation, and it was reported that the predicted values of torsional capacities were within 38% of the experimental values.

In this study, the objective was to obtain more information about RC beams strengthened with externally bonded CFRPs and subjected to torsion. To develop a FE model that can be used to numerically predict the torsional response before and after cracking of FRP-wrapped RC beams and their mode of failure and damage propagation, we presented the method and requirements of the material parameters identification for a concrete damage plasticity constitutive model. Experimental data available from the literature was used for comparison to establish the validity of the results of FE models.

2. EXPERIMENTAL STUDIES CONSIDERED

2.1 Specimen details and experimental setup

For FE validation, the reported experimental results were taken from other studies. Hii and Al-mahaidi[19] performed an experimental investigation on the torsional behaviors of concrete beams reinforced with FRPs by testing six medium-scale specimens with a rectangular cross-section of 500×350 mm and 2500 mm long. Two specimens had solid cross-sections, while the rest were box-shaped with 50-mm-thick walls. CFRP strip spacings of 0.5 and 0.75 of full beam depth were used. They found that the CFRP increases both cracking and ultimate strength by up to 40% for box sections and 78% for solid sections compared to the base specimens. Three specimens, namely CH1, CS1 and FH075D1, were taken from that study as a part of validation of the numerical model in this study. Geometrical details of these specimens are shown in Figure 1.

Another set of specimens was adopted from the study conducted by Chalioris[24]. The authors used an experimental program that included 14 rectangular and T-shaped beams, which were sorted in three groups. All the specimens were tested under pure torsion loading, and eight beams without stirrups were strengthened using CFRP sheets as external transverse reinforcement. Three beams without transverse reinforcement were the control specimens. For comparison purposes, three

beams had steel stirrups as torsional transverse reinforcement. Five specimens, namely Ra-Fs150 (2), Ra-s5.5/75, Rb-c, Rb-F (1) and Rb-S5.5/160, were taken from that study to validate the numerical model. Geometrical details of the tested specimens and the test setup are shown in Figure 2 and 3. In addition, another beam, namely Rc beam, was adopted from the study conducted by Ameli[25] in order to validate damage and failure of numerical model. Merzaei and Tavokkalizadeh[26] conducted pure torsion test on 12 RC beams with a width of 150, a height of 200 and a length of 1500 mm were subjected to a pure torsional loading wrapped by carbon and glass fibers in different configurations. All beams were tested under pure torsion and the torque-twist angle paths of the beams were recorded up to failure. Four beams (B0, B1, B2 and B3) were taken from this research for validation purpose as well. The strengthening configuration is presented in Figure 4. The details of the tested specimens selected for the purpose of numerical simulation are summarized in Table 1. The experimental specimen and torsional test setup meshing is shown in Figure 5.

3. NON-LINEAR FINITE ELEMENT MODELLING

FE modelling of RC beams strengthened with FRP laminates is challenging, as it should correspond with different nonlinear behaviors such as cracking, crushing, yielding of steel, concrete plasticity, FRP deboning, and FRP rupture. Very few studies have focused on the FE study of the behaviors of RC members under torsion.

3.1. Previous researches

Hii and Al-Mahaidi[19] developed a nonlinear FE model to predict the torsional behavior of RC beams under torsion. Nonlinear FE analysis was carried out to experimentally study the tested beams, and the accuracy of the FE to study the torsional behaviors of concrete beams reinforced with FRP composites was verified by ensuring that the torsional strength was reasonably close to

the experimental results in terms of cracking torque, peak torque and torque-twist per unit length response and that the failure mode closely followed the experimental response. Allawi[27] developed a nonlinear FE model to predict the torsional behavior of RC beams under torsion, where the effect of confinement due to the presence of CFRP laminate was taken into consideration to develop constitutive relations for concrete. Ameli et al.[28] proposed FE model for FRP strengthened RC beams. They concluded that the proposed model can efficiently capture cracking and peak torque, but with reasonably less accurate prediction of post-crack stiffness. A nonlinear FE model was proposed in this study to simulate the torsional behavior of concrete beams reinforced with FRP laminates for various parameters using ABAQUS. Modelling details are discussed in the following sections in detail.

3.2. Materials Idealization

Concrete

Concrete is a non-homogeneous quasi-brittle material exhibiting nonlinear behavior. Modelling the exact material behavior is very important in an FE modeling. In all FE simulations discussed hereafter, concrete is modelled using 8-node solid brick elements (C3D8R) with three translational degrees of freedom at each node (directions of x, y, and z corresponding to length, width, and depth of the beam, respectively). This element is capable of plastic deformation, cracking in three orthogonal directions, and crushing. Discretization of RC beam specimens and test setup using ABAQUS and brick solid element are sown in Figure 5.

Reinforcing Bar

Longitudinal and transverse rebars are modeled with three dimensions and two node truss elements (T2D3). The embedded element technique is used to specify that steel reinforcing elements are embedded in host concrete elements. The ABAQUS program examines the position of nodes of

the embedded element in host elements. If a node of an embedded element lies within a host element, its translated degrees of freedom are constrained to the interpolated values of the corresponding degrees of freedom of the host element. The definition of constraint is straight forward and the ABAQUS default values were used. The meshing of steel reinforcing bars elements using ABAQUS and the bars element is shown in Figure 6.

FRP

FRP laminates are modeled as linear elastic materials and the damage parameters are defined using Hashing damage criteria. The mechanical properties of FRP are reported in Table 2. FRP is modelled using three-dimensional shell elements (S4R). The geometry, node locations, and the coordinate system are shown in Figure 7.

Interaction

Concrete-steel interaction is modelled using embedded region constraint, which is a built-in interaction in ABAQUS. Under torsional loading, the bond slip between concrete and steel can be considered insignificant. Mondal and Prakash[29] investigated the effect of bond slip on torsional behavior of RC bridge columns. They concluded that the effect of bond slip is small under torsional loading and assumption of perfecting bonding is a good approximation.

Two methods can be applied to simulate the mechanical interaction between CFRP and concrete. One is based on mesh of FRP and concrete sharing the same nodes, and the other one involves modeling a quadrilateral interface element between concrete and FRP.[30,31] Perfect bond is assumed to define the interaction between concrete and FRP for simplification and therefore a tie constraint is used. Table 3 summarizes the type of element and material behavior used for all the specimens.

3.3 Materials Modeling

The ABAQUS software was implemented in this study to perform nonlinear FE modeling of RC beams strengthened with FRP laminates under pure torsion. ABAQUS provides three different models to simulate the behaviors of RC elements, namely the smeared crack concrete model, the brittle crack concrete model, and the concrete damaged plasticity model. Out of the three concrete crack models, the concrete damaged plasticity model was selected in the present study to represent complete inelastic behavior of concrete under both tension and compression and its damage characteristics. This model assumes two concrete failure mechanisms: tensile cracking and compressive crushing of the material. The concrete damaged plasticity model will be suitable for the analysis of all types of structures (beams, trusses, shells, and solids) under any load combination.

The plastic damage constitutive model in the ABAQUS is suitable for concrete, and it can simulate tensile cracking and compressive crushing of concrete materials based on mechanical properties of concrete under tension and compression. In this model, the uniaxial tensile and compressive behavior is characterized by damaged plasticity.

Concrete

Isotropic and linear elastic behaviors of concrete under compression and tension are defined using Young's modulus and Poisson's ratio. Nonlinear behavior is defined in terms of inelastic strain and corresponding yield stress. Parabolic model is used to define the compressive stress strain curve. The constitutive equations for multiaxial stress state are based on modifications to the concrete uniaxial stress–strain curve. The Hognestad's parabola[32,33] describes the stress–strain response of a normal strength cylinder loaded under uniaxial compression. A nonlinear stress-strain model, proposed by Kent and Park[34], is used to simulate concrete's uniaxial compressive behavior. The model was selected due to its capability to describe the effects of reinforcement

confinement on concrete compressive behavior. The model consists of two parts: a non-linear ascending curve and a linear descending portion. The first part, which is identical for confined and un-confined concrete, describes the stress-strain behavior for stresses up to the maximum compressive stress ($\mathbf{f_c'}$) at the accompanying strain of 0.002. The descending linear portion continues until concrete crushing, which is assumed to occur at 20% of $\mathbf{f_c'}$. The stress strain curve of partially confined concrete has been investigated by several researchers in the past.[35-37] The concrete behavior in uniaxial loading in compression and tension are presented in Figure 8 and 9, respectively.

Definition of concrete damage plasticity in ABAQUS

For defining the behavior of concrete by using concrete damage plasticity in ABAQUS, three main factors should be considered including plasticity, compressive behavior and tensile behavior. The data regarding compressive and tensile behaviors comes from uniaxial compression and uniaxial tension tests, respectively, but the plasticity section needs five parameters including dilation angle, eccentricity, viscosity, biaxial to uniaxial strength ratio $\frac{f_{bo}}{f_{co}}$, and tensile to compressive meridian stresses ratio k_c. Three of these five parameters, including dilation angle, eccentricity and viscosity, have been calibrated in this study and for the two other parameters, the default values have been used. In this study, we considered $\frac{f_{bo}}{f_{co}} = 1.16$ and $k_c = 0.67$, which are typical for concrete and were used in previous studies. Details of a concrete damage plasticity model can be observed in a work conducted by Demin and Fukang[38] and the ABAQUS user's manual.[39] Failure ratios for concrete used in the model are reported in Table 4.

Steel Rebars

In this study, longitudinal and transverse rebars have presumed to have stress-strain relationship under tension and compression as shown in Figure 10. Their behavior before yielding is defined

by Young's modulus and poison ratio. Von Mises yield principle with strain toughening of 0.3 was allocated to the material after yielding.[40]

CFRP Laminates

The tensile behavior of CFRP is considered elastic, as shown in Figure 11. Until tensile strength or rupture strain is reached, the response is considered linear and beyond that tensile failure is recognized. Due to possible micro cracking and delamination, compressive behavior of CFRP can be ignored and therefore a very small Young's modulus in compression were considered. A Poison's ratio of 0.3 to was given to CFRP.

4. RESULTS

FE and experimental results of overall torsional moment behavior were compared for the beams considered from other studies. Analytical predictions were validated with the experimental results obtained from previous studies and a good agreement was found. The details of the test specimens used for validation are summarized in Table 1.

4.1 Ultimate Torque

The observed and predicted values for ultimate torque and the corresponding angle of twist per unit length for each beam are reported in Table 5. The results reflect that the model is able to predict cracking and peak torques with 25% and 12% accuracy, respectively. These errors might be the result of not considering slippage of steel rebars and FRP laminates, premature FRP rupture and FRP debonding that could not be implemented in the FE model. The boundary condition plays a pivotal role in the FE analysis and its result.

4.2 Torque-Twist Behavior

Torque-twist behaviors of all tested beams predicted by the model are presented in Figure 11, displaying the comparison between experimental and FE results of torque-twist behaviors of all

beams considered in this study. In general, it can be noted from the torque-twist curve that the FE analysis is compatible with the experimental results in the full range of behaviors. The FE models accurately predicted cracking torque and cracking twist; also, peak torque and peak twist values were captured reasonably well.

4.3 Crack patterns and failure modes

Crack patterns at failure of the unstrengthened control beams (Rc) and completely wrapped beams with continuous FRP sheets (B1) are presented in Figure 12 and 13. Control beams exhibited typical torsional failure modes with spiral diagonal cracks. Fully wrapped beams with continuous FRP sheets exhibited completely different failure modes since FRP repressed the propagation of cracks (could not be visually observed due to full wrapping). This result explains why fully wrapped beams showed higher values of torsional moment at cracking compared to other beams. Failure usually should start in the most highly stressed fibers followed by the rupture of the part of the FRP laminates that was intersected by the main torsional crack. The mode of failure controlled by the FE model was tested for each beam and compared with the experimental results to ensure the model's accuracy. The damage behavior of the control and FRP strengthened beams was studied, and the comparison of B1 and the reference beam (Rc) is presented to show the difference in the level of damage between strengthened and control beams. The mode of failure predicted by the FE model for all the strengthened beams was FRP rupture at beam corners (due to possible stress concentration) preceded by concrete and matrix cracking and followed by concrete crushing.

The damage state is observed at ultimate load, and it can be noted that the severity level of damage in the FRP strengthened beam (B1) was less than that of its control beam, confirming the contribution of FRP to control the damage and its propagation. It was also observed that FRP

strengthening changed the damage distribution in beams by localizing the damage over a limited area. It can be clearly seen that the presence of FRP reduces the degree of damage in the region. The damage distribution DAMAGEC, PE Max Principal and S Max Principal, which are referred to as compression damage, maximum principal plastic strain and maximum principal stress, respectively are shown in Figure 14 and 15.

5. PARAMETRIC STUDY

A parametric study was carried out to understand the significance of different variables. In addition, the verified FE model was used to study the effect of different limitations on the torsional strength and behavior of concrete beams reinforced with FRP composites to archive more data and provide more information as to the most effective parameters to be considered in design. The limitations were investigated in the parametric study to examine the effect of the number of FRP plies, compressive strength of concrete, and FRP composite strip orientation on torsional capacities.

The concrete compressive strength $\mathbf{f_c'}$ varied from 27.5, 41.25 and 55.0 MPa. The value of $\mathbf{f_c'}$ in the baseline model was 27.5 MPa. Different FRP strip orientation of 45 degrees was considered, while the baseline FRP orientation was 90 degree. The torsional behavior was similar for all models. Beam with $\mathbf{f_c'}$ higher than that of the baseline model had higher values of peak torque relative to the baseline model. Also, there was no significant change in the torque of the RC beam when it was strengthened with a 45 degree FRP laminate. In the case of the number of FRP plies, the FE model corresponding to the experimentally tested strengthened beams (B2) was selected for the baseline comparison. The results presented in Figure 16. Demonstrate that increasing the number of FRP plies caused higher torsional capacity. The FE model for studying compressive strength and FRP composite strip orientation with 45 degrees is shown in Figure 17.

6. CONCLUSION

In this paper, the behaviors of RC beams reinforced with FRP under torsional moment were numerically investigated using an FE software program, and the model was validated with the experimental results from several previous studies. Ultimate torsional moment capacity, torque-angle of twist, cracking pattern and failure mode were evaluated and compared with experimental results to validate the model and determine its accuracy. A parametric study was also conducted to investigate the effect of the number of FRP plies and concrete compressive strength on torsional behavior. According to the results and observations, the following conclusions can be drawn:

- Torsional failure of fully wrapped beams with continuous FRP sheets occurred at higher levels with tensile rupture of the FRP laminates and limited torsional cracking. When using fully wrapped strips to strengthen beams, diagonal cracks formed and widened before final failure with no FRP rupture.
- The nonlinear FE model was able to capture the behavior of RC beams with and without FRP strengthening techniques under pure torsion. The maximum difference in ultimate torque and angle of twist per length were 16% and 35%, respectively. The observed differences between the results from FE models and the experimental findings indicate that the assumption of full interaction of steel rebar and CFRP with concrete is reasonable.
- The nonlinear FE model was capable of displaying damage and failure propagation under torsional loading.
- The parametric study showed that the torsional capacity was enhanced by increasing the number of FRP plies. The use of different numbers of plies of continuous FRP sheets wrapped around the cross-section of rectangular beams along their entire length caused a significant increase in the ultimate torsional strength (between 36% and 55% compared to

the control beam). It was observed that full wrapping with continuous sheets was far more efficient for torsional upgrading.

- The parametric study also showed that RC beams with higher compressive strength displayed higher torsional capacity. Through increasing the concrete compressive strength by 50% and 100%, the torsional capacity elevated by 43% and 86%, respectively. The difference in compressive strength resulted in various failure modes, namely fiber rupture for beams with higher values and crushing of the concrete strut for lower values.
- The study revealed that the concrete damage plasticity model enables a proper definition of the failure mechanisms in concrete elements. This model can be used to replicate the behaviors of concrete, reinforced concrete structures and other pre-stressed concrete structures in advanced loading states.
- The study also serves as a link between the real behavior of concrete and its numerical modelling.

NOTATION

The following symbols are used in this paper:

f'_c = Concrete compressive strength.

b, h = Width and height of cross section.

ε_{fu} = Ultimate tensile strength of FRP laminates.

t_f = Thickness of FRP laminate.

E_{fu} = Elastic modulus of FRP laminates.

$\propto$ = Inclination angle of diagonal crack with respect to the member axis.

β = Inclination angle of FRP strips.

ACKNOWLEDGMENTS

This research was supported by the Faculty of Engineering, Ferdowsi University of Mashhad, under research grant No. 51420. The authors are grateful for the support of the Civil Engineering Department and appreciate the work done by Mr. Mirzaei and staff of the Structures Laboratory.

REFERENCES

1. Ghobarah A, Ghorbel M, Chidiac S. Upgrading torsional resistance of reinforced concrete beams using fiber-reinforced polymer. *Journal of composites for construction.* 2002;6(4):257-263.
2. Täljsten B. Strengthening of concrete structures for shear with CFRP-fabrics: test and theory. Paper presented at: International Conference on Concrete Under Severe Conditions: 21/06/1998-24/06/19981998.
3. Triantafillou T, Matthys S. Fibre-reinforced polymer reinforcement enters fib Model Code 2010. *Structural Concrete.* 2013;14(4):335-341.
4. Mohamed N, Elrawaff B, Abdul Samad AA, Alferjani M. Experimental and theoretical investigation on shear strengthening of rc precraced continuous t-beams using CFRP strips. *International Journal of Engineering.* 2015;28(5):671-676.
5. Kabir MH, Fawzia S, Chan T, Gamage JC, Bai J. Experimental and numerical investigation of the behaviour of CFRP strengthened CHS beams subjected to bending. *Engineering Structures.* 2016;113:160-173.
6. Grammatikou S, Biskinis D, Fardis MN. Flexural rotation capacity models fitted to test results using different statistical approaches. *Structural Concrete.* 2018;19(2):608-624.
7. Khalifa A, Gold WJ, Nanni A, MI AA. Contribution of externally bonded FRP to shear capacity of RC flexural members. *Journal of composites for construction.* 1998;2(4):195-202.
8. Rahal KN. Shear strength of reinforced concrete: Part II—Beams subjected to shear, bending moment, and axial load. *Structural Journal.* 2000;97(2):219-224.

9. Joseph B, Yost R, Goodspeed C, Schmeckpeper E. *F Lexural P Erformance of Concrete With Frp G Rids.* 2001.
10. Liang QQ, Uy B, Bradford MA, Ronagh HR. Strength analysis of steel–concrete composite beams in combined bending and shear. *Journal of Structural Engineering.* 2005;131(10):1593-1600.
11. Bousselham A, Chaallal O. Behavior of reinforced concrete T-beams strengthened in shear with carbon fiber-reinforced polymer-an experimental study. *ACI structural Journal.* 2006;103(3):339.
12. Vora TP, Shah BJ. Experimental investigation on shear capacity of RC beams with GFRP rebar & stirrups. *Steel and Composite Structures.* 2016;21(6):1265-1285.
13. Saadatmanesh H, Ehsani MR, Li M-W. Strength and ductility of concrete columns externally reinforced with fiber composite straps. *Structural Journal.* 1994;91(4):434-447.
14. Fam A, Flisak B, Rizkalla S. Experimental and analytical modeling of concrete-filled FRP tubes subjected to combined bending and axial loads. *ACI Struct J.* 2003;100(4):499-509.
15. Prashob P, Shashikala A, Somasundaran T. Behaviour of carbon fiber reinforced polymer strengthened tubular joints. *Steel and Composite Structures.* 2017;24(4):383-390.
16. Fanaradelli T, Rousakis T. Assessment of analytical stress and strain at peak and at ultimate conditions for fiber-reinforcement polymer-confined reinforced concrete columns of rectangular sections under axial cyclic loading. *Structural Concrete.* 2020.
17. Panchacharam S, Belarbi A. Torsional behavior of reinforced concrete beams strengthened with FRP composites. Paper presented at: First FIB Congress, Osaka, Japan2002.
18. Salom PR, Gergely J, Young DT. Torsional strengthening of spandrel beams with fiber-reinforced polymer laminates. *Journal of Composites for Construction.* 2004;8(2):157-162.
19. Hii AK, Al-Mahaidi R. An experimental and numerical investigation on torsional strengthening of solid and box-section RC beams using CFRP laminates. *Composite structures.* 2006;75(1-4):213-221.

20. Souza OLdC, Sánchez Filho EdS, Vaz LE, Silva Filho JJH. Reliability analysis of RC beams strengthened for torsion with carbon fibre composites. *Structural Concrete.* 2014;15(1):38-44.
21. Majeed AA, Allawi AA, Chai KH, Badaruzzam HW. Behavior of CFRP strengthened RC multicell box girders under torsion. *Structural Engineering and Mechanics.* 2017;61(3):397-406.
22. Sakin S, Anil Ö. Nonlinear finite element model for interface between anchoraged carbon fiber reinforced polymer and concrete surface. *Structural Concrete.* 2019;20(6):1986-1999.
23. Alabdulhady MY, Sneed LH. Torsional strengthening of reinforced concrete beams with externally bonded composites: A state of the art review. *Construction and Building Materials.* 2019;205:148-163.
24. Chalioris CE. Torsional strengthening of rectangular and flanged beams using carbon fibre-reinforced-polymers–Experimental study. *Construction and building materials.* 2008;22(1):21-29.
25. Ameli M, Ronagh H, Dux P. Experimental investigations on FRP strengthening of beams in torsion. 2005.
26. Mirzaei Hesari H, Tavakkolizadeh M. Torsional reinforcement of rectangular reinforced concrete beams using FRP using grooving and reciprocating methods. Paper presented at: the 9th National Concrete Conference of Tehran, Iran2018.
27. Allawi A. *Nonlinear analysis of reinforced concrete beams strengthened by CFRP in torsion*, Ph. D. Thesis, University of Baghdad; 2006.
28. Ameli M, Ronagh HR, Dux PF. Behavior of FRP strengthened reinforced concrete beams under torsion. *Journal of Composites for Construction.* 2007;11(2):192-200.
29. Mondal TG, Prakash SS. Nonlinear finite-element analysis of RC bridge columns under torsion with and without axial compression. *Journal of Bridge Engineering.* 2016;21(2):04015037.
30. Al-Mahaidi R, Hii AK. Bond behaviour of CFRP reinforcement for torsional strengthening of solid and box-section RC beams. *Composites Part B: Engineering.* 2007;38(5-6):720-731.

31. Obaidat YT, Heyden S, Dahlblom O. The effect of CFRP and CFRP/concrete interface models when modelling retrofitted RC beams with FEM. *Composite Structures.* 2010;92(6):1391-1398.
32. Hognestad E. *Study of combined bending and axial load in reinforced concrete members.* University of Illinois at Urbana Champaign, College of Engineering …;1951.
33. Hognestad E, Hanson NW, McHenry D. Concrete stress distribution in ultimate strength design. Paper presented at: Journal Proceedings1955.
34. Kent DC, Park R. Flexural members with confined concrete. *Journal of the Structural Division.* 1971.
35. Scott BD, Park R, Priestley MJ. Stress-strain behavior of concrete confined by overlapping hoops at low and high strain rates. Paper presented at: Journal Proceedings1982.
36. Mander JB, Priestley MJ, Park R. Theoretical stress-strain model for confined concrete. *Journal of structural engineering.* 1988;114(8):1804-1826.
37. Chakrabortty A, Khennane A. Failure mechanisms of hybrid FRP-concrete beams with external filament-wound wrapping. *Advances in concrete construction.* 2014;2(1):057.
38. Demin W, Fukang H. Investigation for plastic damage constitutive models of the concrete material. *Procedia engineering.* 2017;210:71-78.
39. Hibbitt, Karlsson, Sorensen. *Abaqus/CAE User's Manual.* Hibbitt, Karlsson & Sorensen, Incorporated; 2002.
40. Obaidat Y. Structural retrofitting of reinforced concrete beams using carbon fiber polymer. *Licentiate dissertation, Structural Mechanics, Lund, Sweden, ISSN.* 2010:0281-6679.

TABLE 1. Details of the specimens used in other studies

Beam	**b, h mm**	**ε_{fu} $\times 10^{-3}$**	**f'_c MPa**	**t_f mm**	**E_{fu} GPa**	**$\propto$ Deg**	**β Deg**	**Strengthening Configuration**
CH1[19]	500, 350	-	48.9	-	-	-	-	Control beam(box)
CS1[19]	500, 350	-	52.5	-	-	-	-	Control beam(solid)
FH075D1[24]	500, 350		48.9	0.176	240	45	90	Full strips(box)
Ra-Fs150(2)[24]	100, 200	1.5	27.5	0.110	230	45	90	Strips with 150 mm width 300 mm apart
Ra-s5.5/75[24]	100, 200	-	27.5	-	-	-	-	Without FRP
Rb-c[24]	150, 300	-	28.5	-	-	-	-	Without FRP
Rb-F(1)[24]	150, 300	1.5	28.5	0.050	230	45	90	Full wrapping
Rb-S5.5/160[24]	150, 300	-	28.5	-	-	-	-	Without FRP
Rc[25]	150, 350	-	39.0	-	-	-	-	Without FRP
B0[26]	150, 200	-	35.0	-	-	-	-	Control beam
B1[26]	150, 200	1.5	35.0	0.110	230	45	90	Fully and completely wrapped beams with continuous CFRP sheets
B2[26]	150,200	1.5	35.0	0.110	230	45	90	U-wrap beams with CFRP
B3[26]	150,200	1.5	35.0	0.110	230	45	90	Wrapping with75 mm width strips spaced 110mm

TABLE 2. Mechanical properties of the unidirectional carbon FRP laminates

Mechanical Property	CFRP Sheet
Longitudinal tensile modulus, E_1 (GPa)	120
Transverse modulus, E_2 (GPa)	2
Shear modulus, G_{12} (GPa)	5.8
Poisson ratio, υ_{12} (GPa)	0.27
Longitudinal tensile strength, X_T (MPa)	2160
Transverse tensile strength, Y_T (MPa)	50
Longitudinal compressive strength, X_C (MPa)	702
Transverse compressive strength, Y_C (MPa)	133
Shear strength, S (MPa)	75

TABLE 3. Element type and idealized stress strain curve of the materials

Material	**Element type**	**Idealized relationship**
Concrete	Solid-C3D8R	Parabolic
Steel	Truss-T2D3	Elastoplastic
FRP	Shell-S4R	Elastic

TABLE 4. Damage parameters of concrete damage plasticity model for concrete

Damage Parameters	**Failure Ratio**
Dilation angle	36
Eccentricity	0.1
f_{bo}/f_{co}	1.16
K	0.67
Viscosity parameter	0.002

TABLE 5. Experimental and numerical results for the control and strengthened beams under pure torsion

Specimen	**Cracking torque T_c (kN-m)**		**Cracking twist θ_c (rad/m)**		**Peak torque T_u (kN-m)**		**Peak twist θ_u (rad/m)**		$\frac{T_{u,FEM.}}{T_{u,EXP.}}$	$\frac{\theta_{u,,FEM.}}{\theta_{u,EXP.}}$
	EXP.	FEM.	EXP.	FEM.	EXP.	FEM.	EXP.	FEM.		
CH1[19]	15.80	30.87	0.030	0.31	49.40	48.99	5.29	6.17	0.99	1.16
CS1[19]	68.4	58.15	0.15	0.26	62.9	71.38	1.79	1.2	1.13	0.76
FH075D1[24]	19.60	20.86	0.000	0.090	67.50	61.05	4.6	4.8	0.9	1.04
Ra-Fs150(2)[24]	2.20	1.76	0.009	0.006	3.01	3.04	0.088	0.076	1	0.86
Ra-s5.5/75[24]	2.25	2.23	0.013	0.008	3.15	2.94	0.078	0.052	0.9	0.66
Rb-c[24]	6.951	7.36	0.010	0.0079	6.951	7.36	-	-	1.05	-
Rb-F(1)[24]	8.79	8.77	0.009	0.007	10.05	10.27	0.071	0.052	1.02	0.73
Rb-S5.5/160[24]	6.92	7.66	0.009	0.008	6.92	7.66	0.009	0.008	1.1	0.88
Rc[25]	-	-	-	-	15.00	13.89	5.2	5.34	0.92	1.02
B0[26]	3.30	2.70	1.000	0.530	3.87	3.61	4	4.29	0.93	1.07
B1[26]	4.00	5.36	0.005	0.0.06	14.16	11.93	0.11	0.123	0.84	1.11
B2[26]	3.76	3.26	1.300	0.630	5.41	4.95	5.2	5.4	0.91	1.03
B3[26]	3.8	5.23	0.011	0.012	6.66	6.90	0.1	0.065	0.96	0.65

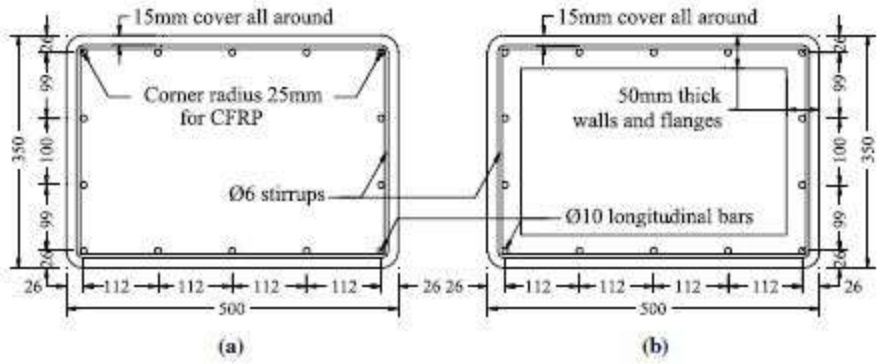

FIGURE 1. Reinforcement details of the tested specimens: (a) solid section and (b) hollow section[19]

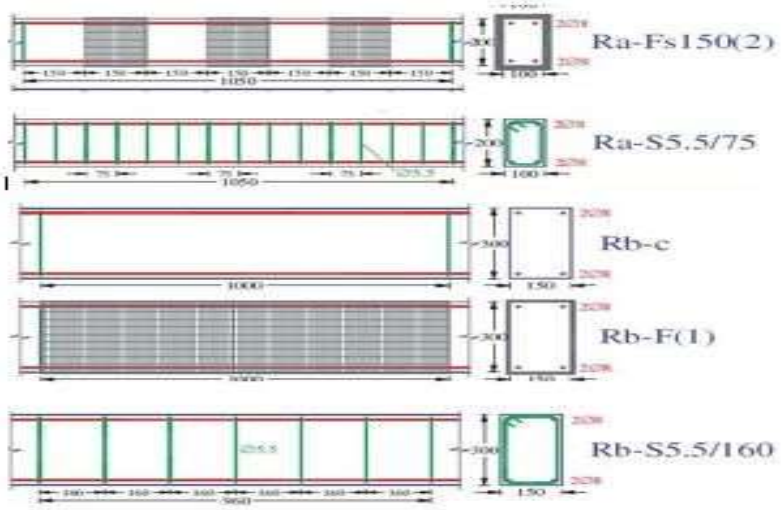

FIGURE 2. Geometry and reinforcement arrangement of the tested specimens[24]

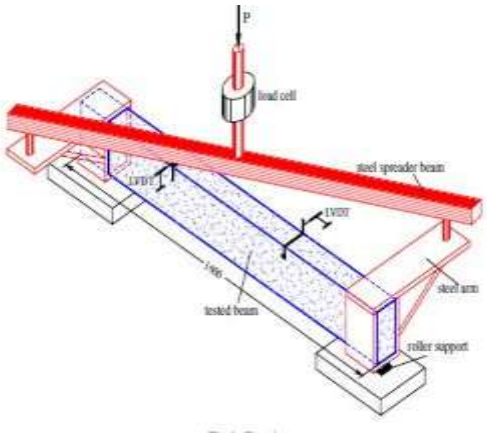

FIGURE 3. Pure torsion test setup[24]

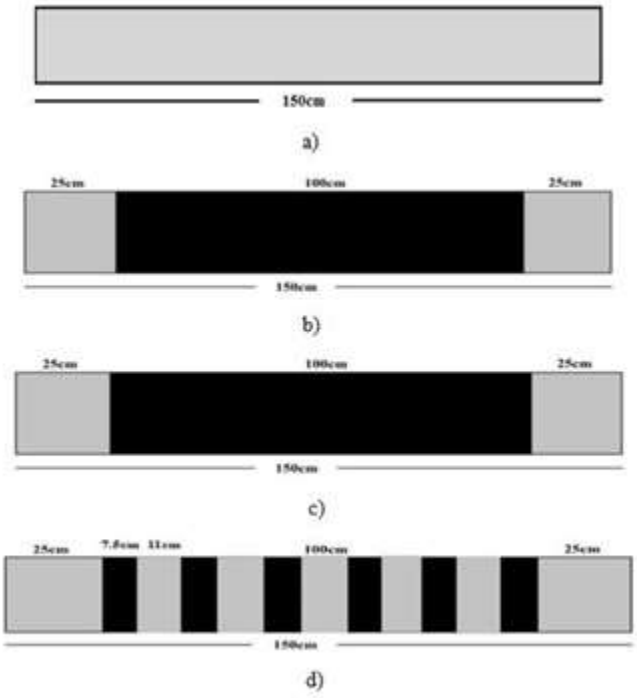

FIGURE 4. Geometry and reinforcement arrangement of the tested beam: (a) control beam, (b) complete wrap, (c) U-wrap, and (d) wrapping with strips[26]

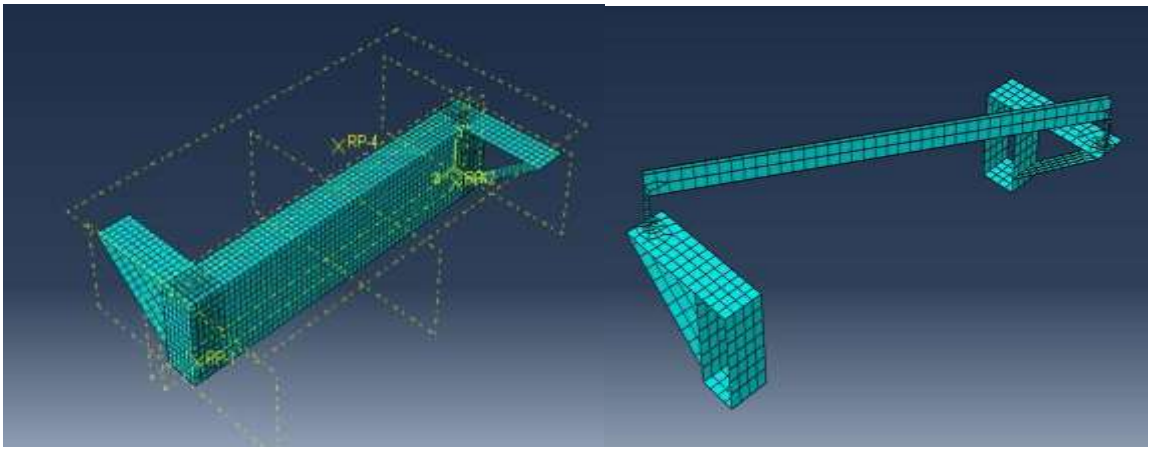

FIGURE 5. Meshing of concrete specimen and torsional test setup

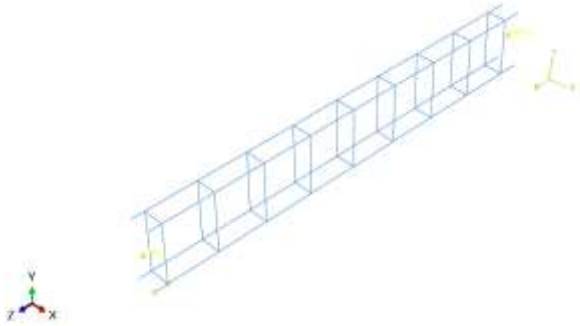

FIGURE 6. Meshing of longitudinal and transverse steel rebars

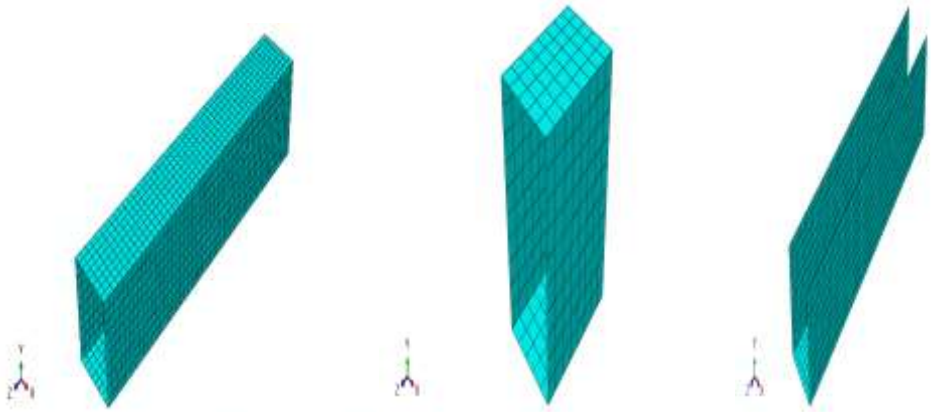

FIGURE 7. Meshing of FRP laminate (full, stirrup and U wrapping)

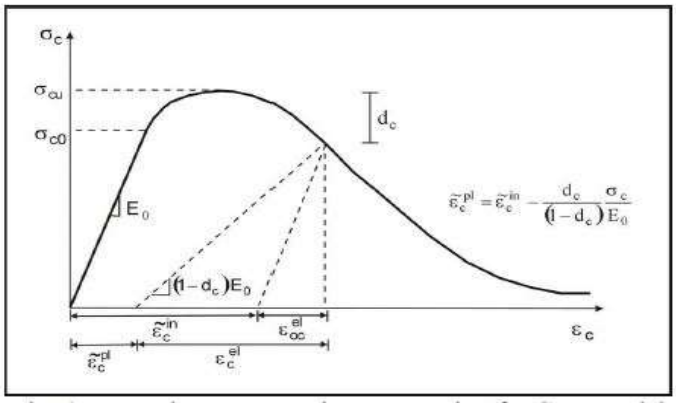

FIGURE 8. Response of concrete to uniaxial loading in compression[39]

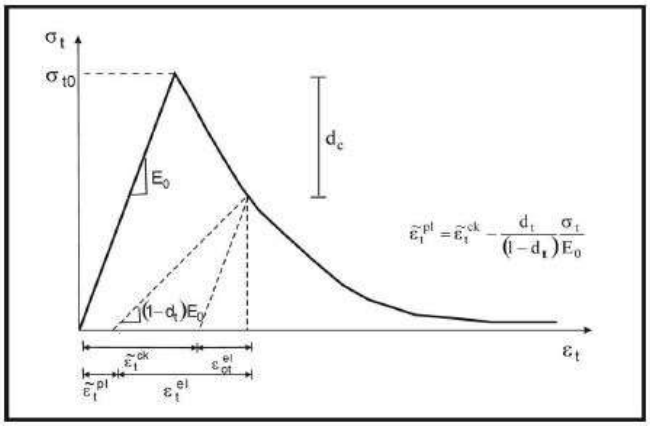

FIGURE 9. Response of concrete to uniaxial loading in tension[39]

`

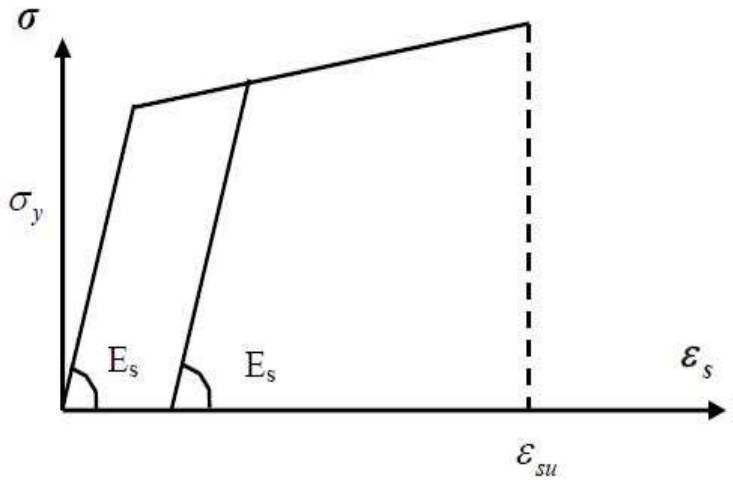

FIGURE 10. Stress-Strain relationship of steel rebars[27]

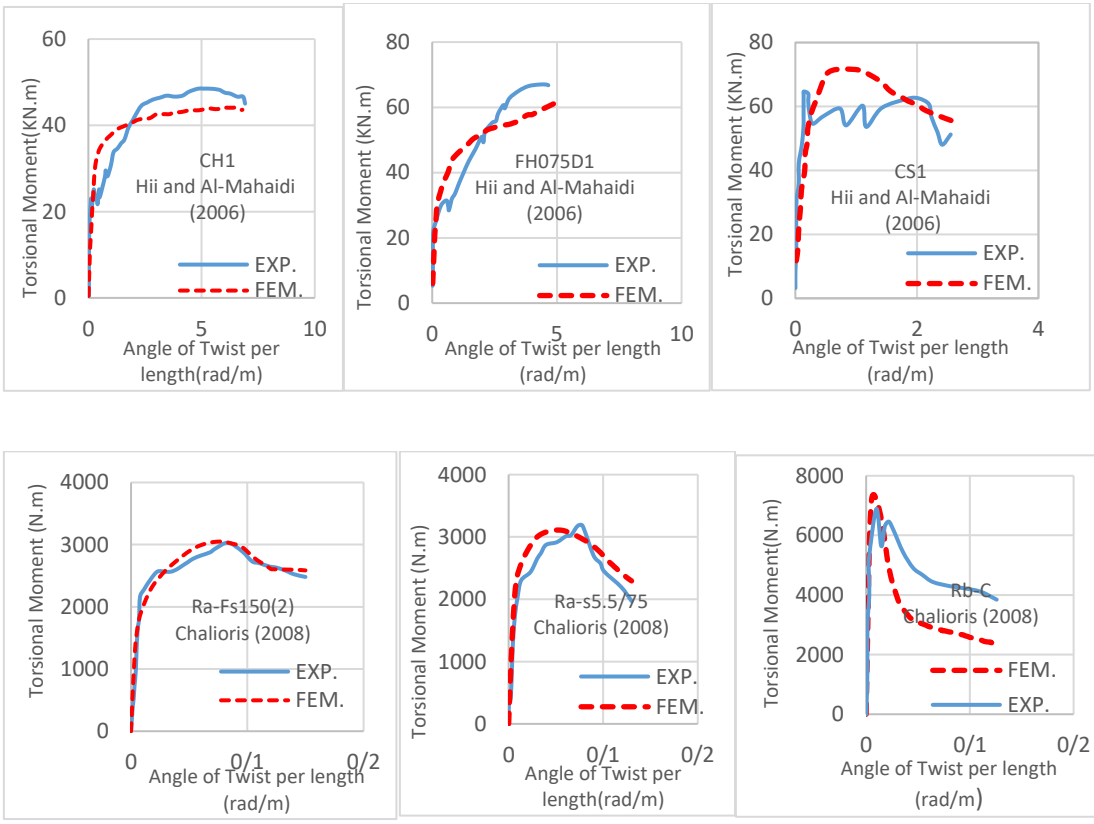

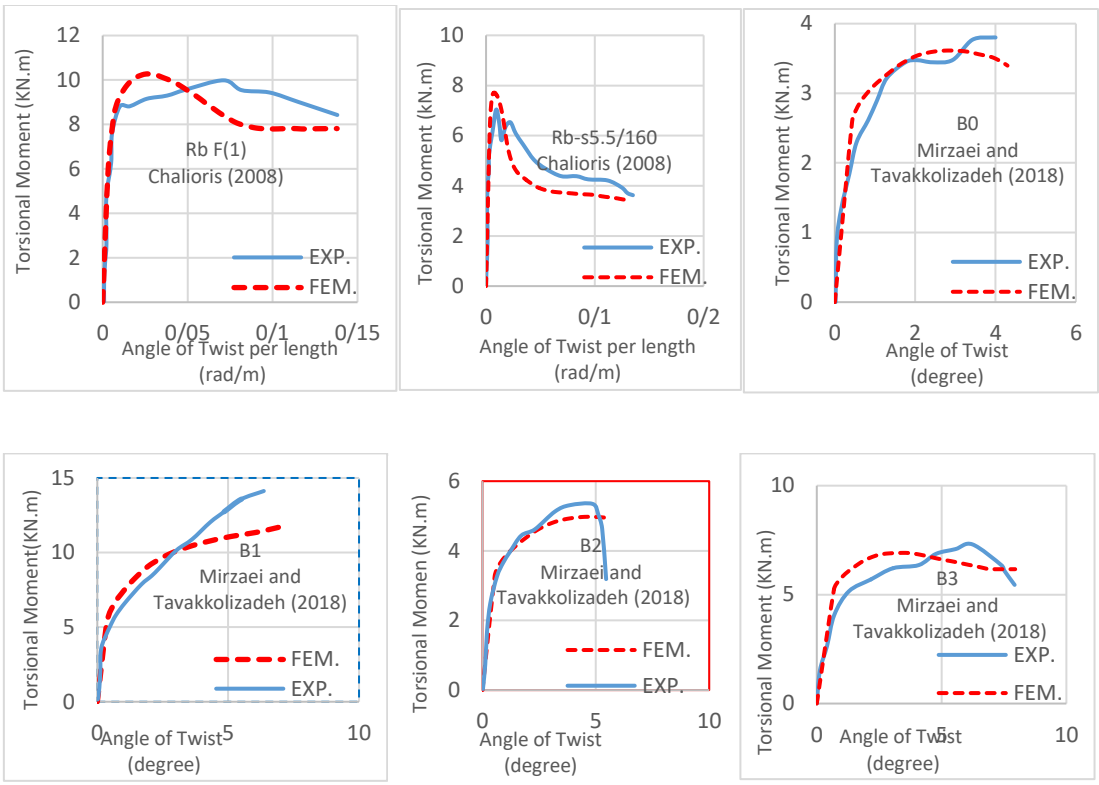

FIGURE 11. Comparison of the finite element method results with experimental data

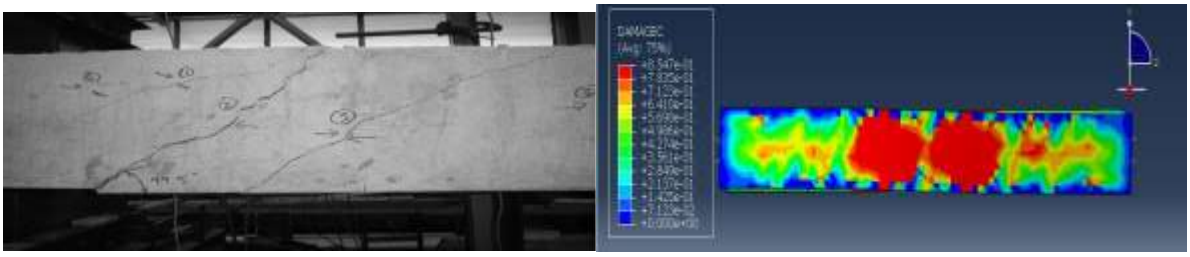

Crack patterns of control beams (Exp.) Crack patterns of control beams (FEM)

FIGURE 12. Effect of damage distribution on torsion control specimen (Rc)[25]

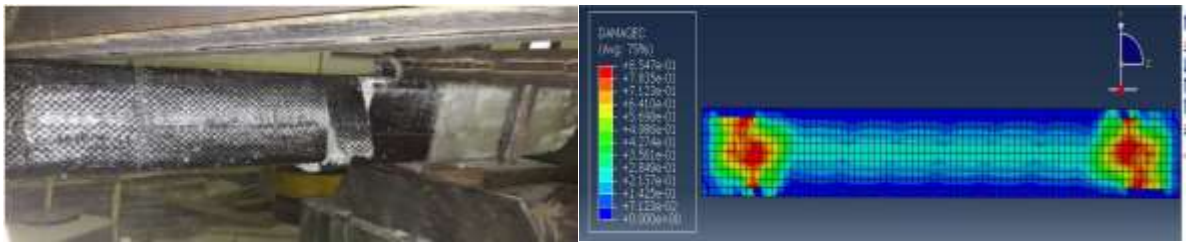

Crack patterns of control beams (Exp.) Crack patterns of control beams (FEM)

FIGURE 13. Effect of damage distribution on torsion control specimen (B1)[26]

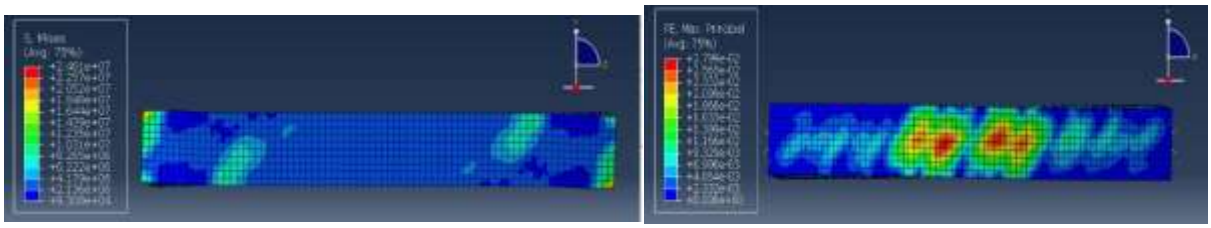

Principal stress Principal plastic strain

FIGURE 14. Maximum principal stress and plastic strain for unstrengthened RC beam [B0][26]

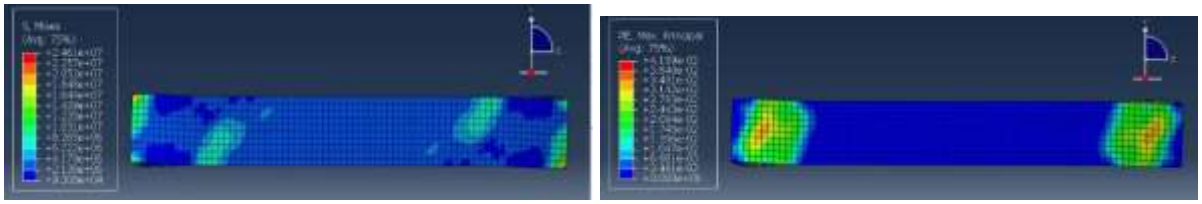

Principal stress Principal plastic strain

FIGURE 15. Maximum principal stress and plastic strain for fully wrapped RC beam [B1][26]

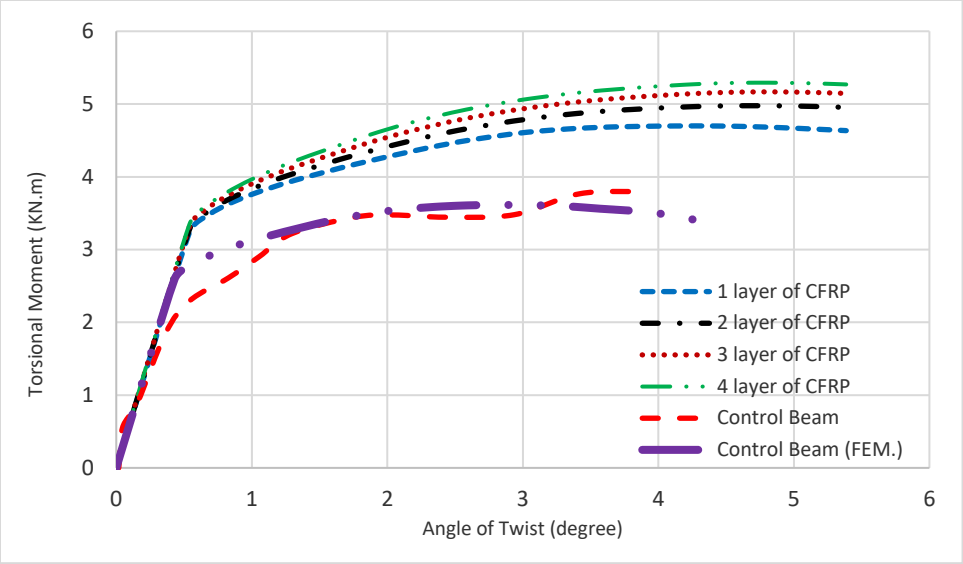

FIGURE 16. Numerical and experimental torque-twist behavior of specimen (B2)[26] with different number of plies

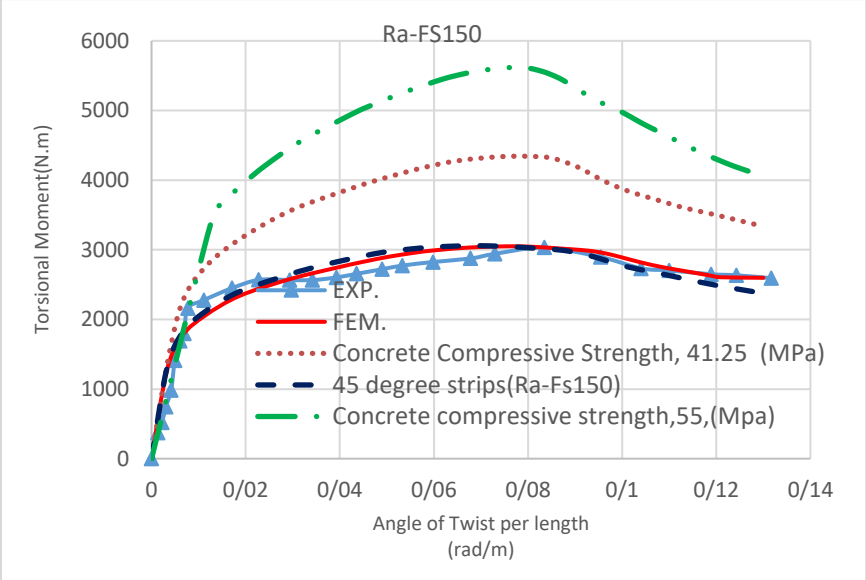

FIGURE 17. Numerical and experimental torque-twist behavior of specimen (Ra-Fs150(2))[24] for different concrete compressive strengths